Asian Journal of Chemistry; Vol. 33, No. 9 (2021), 2007-2014

ASIAN JOURNAL OF CHEMISTRY

https://doi.org/10.14233/ajchem.2021.23260

Synthesis of Zirconia Doped Molybdenum Oxide as Efficient Catalysts for Ultrasound Assisted Synthesis of Substituted Pyrazoles

AMAL A. MUFTAH[1], SHOBHA A. WAGHMODE[2] and SHARDA R. GADALE[3,*]

[1]Faculty of Education, Bani Walid University, Bani Walid, Libya
[2]Department of Chemistry, Abasaheb Garware College, Pune-411004, India
[3]Department of Chemistry, Yashwantrao Mohite College of Arts Science and Commerce, Bharati Vidyapeeth (Deemed To Be University), Pune-411038, India

*Corresponding author: E-mail: dagade@rediffmail.com

Received: 22 April 2021; *Accepted*: 5 June 2021; *Published online*: 20 August 2021; AJC-20456

To explore green methodology for the synthesis of mixed oxide, its catalytic activity and temperature stability of series of ZrO_2/MoO_3 and ZrO_2 were prepared by sol-gel method and characterized by XRD, FT-IR, X-ray photoelectron spectroscopy (XPS), temperature programmed Desorption (TPD), Raman spectroscopy and transmission electron microscopes (TEM). These mixed oxides were showed high stability with nanocrystalline nature. Due to highly acidic nature of the catalysts, ultra sound assisted synthesis of substituted pyrazoles was carried out successfully with high yield. The reaction was carried out in solvent free medium, which showed green approach and energy saving reaction. Condensation of dibenzoyl methane and hydrazine to form substituted pyrazoles with 97.7% yield. The acid strength and acid amount of synthesized catalysts were determined by temperature programmed desoprtion (TPD), incorporation of zirconia into the molybdenum, network has changed its surface acid properties due to the Zr^{2+} and Mo^{6+} ions. After addition of ZrO_2 on MoO_3, it showed weak and strong acid sites.

Keywords: Zirconia, Mixed oxide, Thermal stability, Sol-gel, Pyrazoles, Green technology, Innovation.

INTRODUCTION

Solid acids have been the important subjects owing to their applications in many chemical industries with different advantages, which include simplicity, easy handling and versatility of process engineering, catalyst regeneration and plant corrosion problems and environmental safe disposal. A number of organic syntheses as well as transformation reactions have been conducted with mixed oxides leading which depend on the strength of the acid and type of acidity [1,2]. The different optical, magnetic, physical and chemical properties of metal oxides are of great importance due to their extremely sensitive to changes in composition and structure. Transition metal oxides are attracting special attention because of their multi-functional behaviour [3-7].

Over the past few decades, zirconium oxide has obtained interest as both, supported catalyst such as ZrO_2/Li_2O, ZrO_2/SiO_2, WO_3/ZrO_2, Ru/W/ZrO_2, series of MoO_3/ZrO_2-Al_2O_3 catalysts and as a single oxide, mostly due to having both acid and base sites, and stability under oxidizing and reducing atmospheres [8-12].

Few researchers [13-17] synthesized various combinations of ZrO_2 mixed oxides such as CrO_x-ZrO_2, ceria-zirconia-alumina, nanoparticles of tetragonal zirconia, CeO_2-ZrO_2 by different methods like sol-gel and co-precipitation. These mixed oxides were characterized by various techniques to understand thermal stability, effect of zirconia and other factors.

The molybdenum doped on zirconia has been studied by few researchers [18-20] and were prepared by facile hydrothermal, sol-gel and co-precipitation method. The obtained supports showed tetragonal zirconia phase as well as monoclinic zirconia. Seyed *et al.* [21] reported the pyrazole synthesis with green media PEG-400 and water combination and brought higher yield under ultrasound irradiation.

This article is focused on the catalytic activity of prepared catalysts on the condensation of dibenzoyl methane and hydra-

zine to form substituted pyrazoles with higher yield under ultrasound. This method gives greener approach with solvent-free reaction. The structural stability of zirconia supported on the molybdenum oxides was also studied, as most of the researchers worked on MoO_3 supported on different metal oxide oxides such as ZrO_2, WO_2/ZrO_2, CeO_2-ZrO_2, TiO_2-ZrO_2, MoO_3-ZrO_2 but ZrO_2 supported on MoO_3 as a binary oxide composition is not studied for the catalytic applications [22]. As ZrO_2 has dispersed on surface of MoO_3, it indicated that acidic and basic sites are more available for the surface reaction.

EXPERIMENTAL

Catalyst preparation: Sol-gel method were used for the synthesis of ZrO_2 supported on MoO_3 (ZM) with different zirconium loading 1 wt.% and 10 wt.%. Zirconyl nitrate and ammonium heptamolybdate were used as zirconium and molybdenum source. In typical procedure, 1 wt.% ZrO_2/MoO_3 (1ZM) catalyst was synthesized by dissolving of ammonium heptamolybdate in distilled water by heating for 30 min, followed by the addition of isopropyl alcohol under stirring. Then fixed amount of zirconyl nitrate was added slowly to the above solution with stirring till gel formed. This resultant transparent gel, air dried then calcined at 500, 600 and 700 ºC in a muffle furnace for 5 h. By similar procedure 10 ZM was prepared.

Characterization: The crystallite size of the samples was determined by X-ray power diffraction (XRD) using Rigaku Ultima IV diffraction using Cu*K*α radiation and a Ni filter. The FT-IR spectra were recorded on Thermo Nicolet iS5 IR instrument at ambient conditions using KBr pellets with a resolution of 4 cm^{-1} in the range of 4000-400 cm^{-1} and with 32 scans. X-ray photoelectron spectroscopy (XPS) studies were carried out on a VSW scientific instrument using incident source with an energy of 1253 eV and a resolution of 0.9 eV vacuum of 10^{-8} torr was maintained in the sample analyzer chamber. The temperature-programmed desorption (TPD) was used for the determination of degree of acidity of the samples using NH_3 as molecule.

RESULTS AND DISCUSSION

XRD studies: The XRD patterns of pure ZrO_2 and 1 wt.% and 10 wt.% ZrO_2/MoO_3 are presented in Fig. 1. The pure ZrO_2 catalyst showed intense peaks at 2θ = 30.22º, 35.0º, 50.31º and 60.12º corresponding to tetragonal phase of ZrO_2 with planes (101), (110), (112) (211), respectively and confirmed with JCPS file no.17-0923. The average crystallite size for pure ZrO_2 was calculated to be 16 nm based on Debye equation.

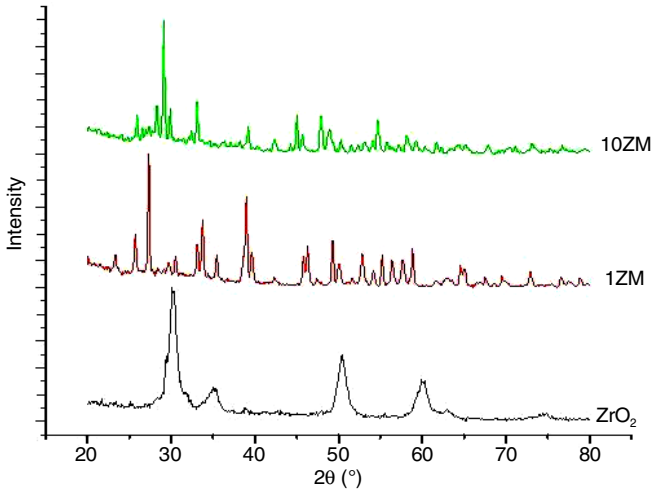

Fig. 1. XRD pattern of ZR, 1ZM and 10 ZM catalysts calcined at 500 °C

The prepared ZrO_2/MoO_3 (ZM) mixed oxide were showed characteristic peak for α-MoO_3 at 23.4º, 25.8º, 27.4º, 33.7º and 49.6º. The obtained XRD peaks confirmed the formation of tetragonal ZrO_2 over the surface of MoO_3 support and it can be observed that the loading of ZrO_2 over MoO_3 increased, then there was hindrance of support and due to support, crystallite size was reduced slightly [23].

The effect of calcination temperature was studied on prepared catalysts to know the stability of phases present in them. XRD pattern of samples calcined at different temperatures are shown in Fig. 2. As-synthesized ZrO_2 (ZR) and ZM samples

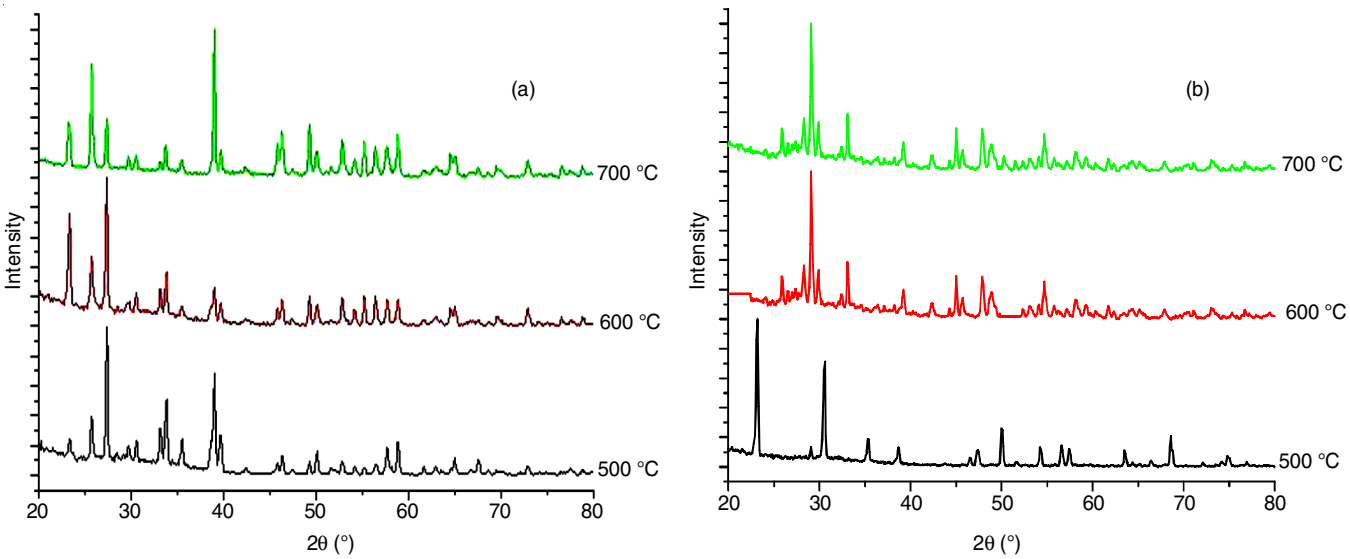

Fig. 2. XRD patterns of 1ZM (a) and 10ZM (b) catalysts calcined at different temperatures

calcined at 500 ºC was observed in tetragonal phase. As temperature increased from 500 to 700 ºC, tetragonal phase changed to mixture of tetragonal and monoclinic phase was observed in ZR and ZM samples.

From the results, it was concluded that the small size of the particles is responsible for the stabilization of the tetragonal phase and established fact that tetragonal phase is more active in catalysis as reported and explained in literature [1]. Therefore, it is evident that the thermal stability of zirconia is highly dependent on the calcination temperature.

Crystallite size of samples was calculated by Debye-Scherrer equation. The effect of calcination temperature on crystallite size is shown in Table-1. All the synthesized catalysts were in nanosized having crystallite size in range between 7.0-17.3 nm.

TABLE-1
EFFECT OF CALCINATION TEMPERATURE ON CRYSTALLITE SIZE OF SYNTHESIZED CATALYSTS

Catalyst	Calcination temperature (°C)	Crystallite size (nm)
Pure ZrO_2	500	16.50
	600	16.99
	700	17.30
1ZM	500	7.00
	600	7.34
	700	7.70
10ZM	500	7.40
	600	7.60
	700	7.90

FTIR studies: The FTIR spectra of pure zirconia and ZM samples are shown in Fig. 3. The FTIR data of ZrO_2 sample showed different peaks at 740, 1100, 1380 and 2170 cm^{-1}. The peak at 545 cm^{-1} corresponds to Zr-O stretching modes and peak at 740 cm^{-1} due to Zr-O_2-Zr asymmetric which confirm the formation of ZrO_2 Phases [4]. Wang *et al.* [8,11] also reported the same observations for zirconia catalyst. In ZrO_2/MoO_3 samples, the same peak for ZrO_2 at 740 cm^{-1} was observed along with the peaks at 870 and 1000 cm^{-1} which corresponds to α-MoO_3 stretching mode [6].

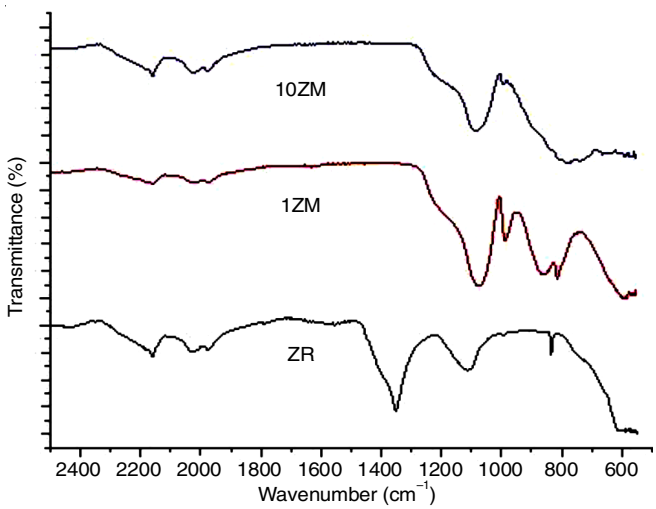

Fig. 3. FT-IR Spectra of pure ZrO_2 and various % ZM samples

Raman studies: Raman spectra of pure ZrO_2 and various % ZM catalysts calcined at 500 ºC ae shown in Fig. 4. Pure ZrO_2 catalyst showed the peaks at 164, 270, 310, 466 and 624 cm^{-1}, which correspond to the theoretical bands for tetragonal phase of zirconia [9]. The mixed oxide ZM catalysts showed peaks for tetragonal phase of $ZrO_2$with slightly increasing of intensity might due to Zr-Mo interaction. The spectra of ZM showedpeaks of α-MoO_3 at 161, 285, 293, 339, 381, 666, 819 and 996 cm^{-1} as per the reported in literature [10]. There was shift in peaks took place with increasing of zirconia loading from 1% to 10%. This may be due to the effect of zirconia loading. In case of 10ZM, a sharp peak of polymolybdate was observed at 890 cm^{-1} and not observed in 1ZM. As samples were calcined at 500 ºC, so there was no peaks observed for β-MoO_3 which signified the selective decomposition of molybdate to the α-MoO_3 occurs.

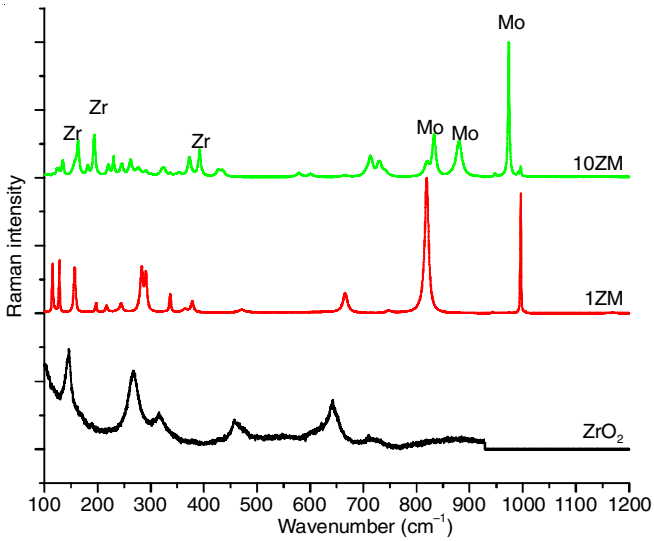

Fig. 4. Raman spectra of ZrO_2, 1ZM and 10ZM catalysts from 0.043 to 0.08 mmol/g

Temperature programmed desoprtion (TPD) studies: The TPD spectra of ZrO_2 is shown in Fig. 5a. The results showed the strong desorption peak at around 692 ºC, it is generally reported that the surface acidity of zirconia catalyst is due to surface Zr^{2+} species and OH^- species. As seen in Fig. 5b-c, the addition of ZrO_2 into molybdenum lattice changed its surface acidic properties due to Zr^{2+} and Mo^{6+} ions. The desorption of 1% ZrO_2/MoO_3 catalyst shows two peaks, one at higher intensity (636.1 ºC) and other at lower intensity (220 ºC), which showed acidity up to 0.043 mmol/g. In the earlier report [24], molybdenum showed only weak acid sites in low temperature region, therefor after incorporation of zirconia on MoO_3, it showed weak and strong acid sites. While the TPD spectra of 10%ZrO_2/MoO_3 showed sharp peak at high intensity (533 ºC) as shown in Fig. 5c. As the concentration of ZrO_2 increased from 1% to 10%, the total acidity increased from 0.043 to 0.08 mmol/g as shown in Table-2. Thus, as the concentration of ZrO_2 increased from 1 wt.% to 10 wt.%, the total acidity increased from 0.043 to 0.08 mmol/g.

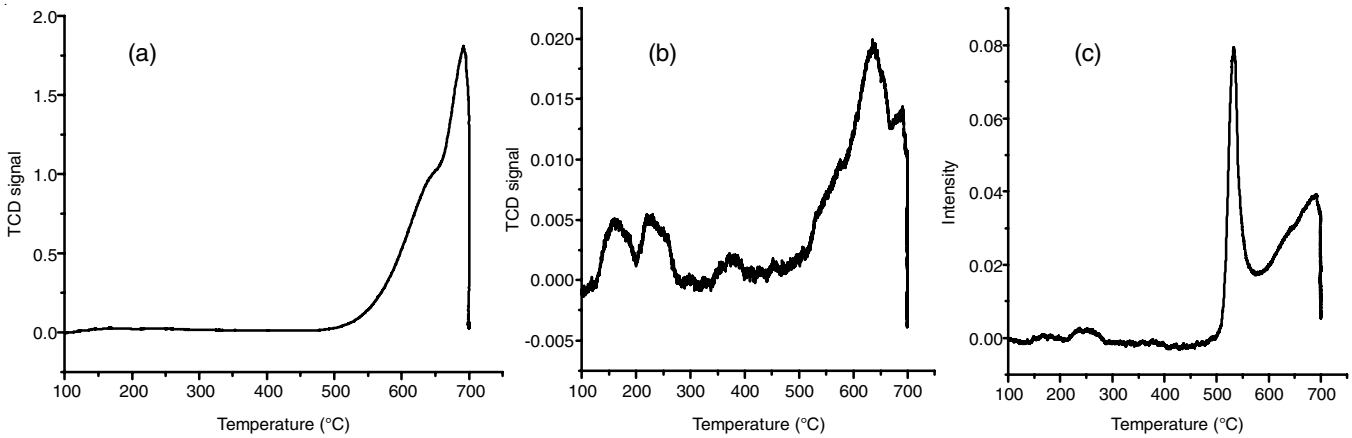

Fig. 5. TPD spectra of (a) ZrO_2, (b) 1ZM and (c) 10ZM samples calcined at 500 °C

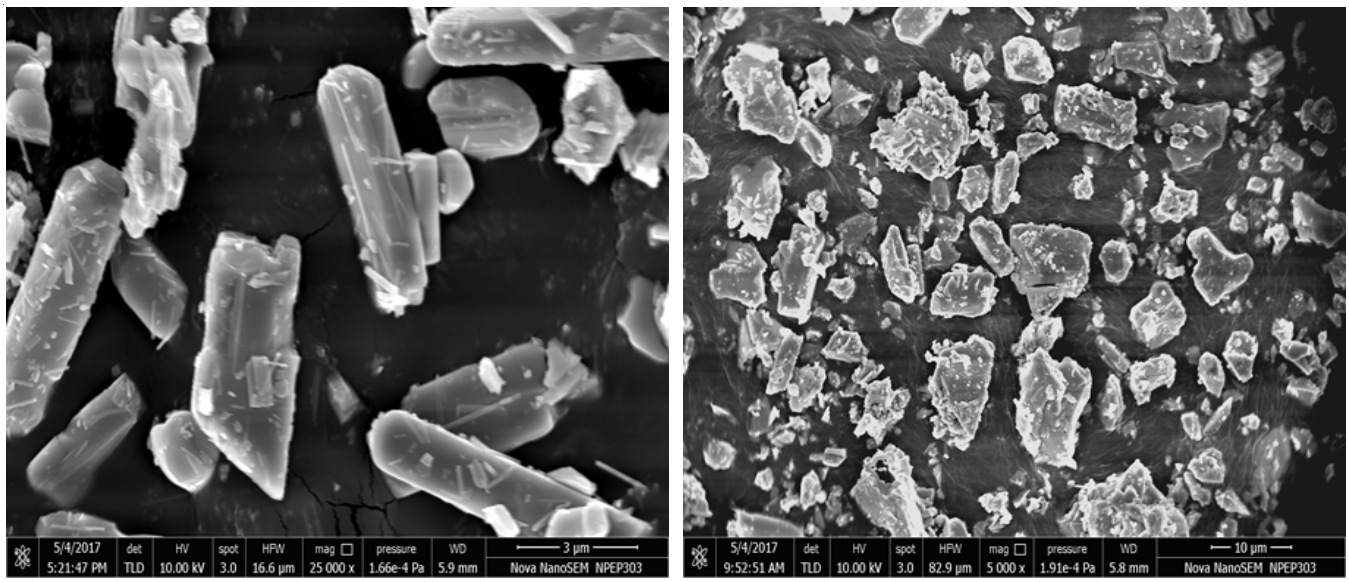

Fig. 6. FESEM images of 1ZM and 10ZM samples

TABLE-2
ACIDITY MEASUREMENT OF THE PREPARED CATALYSTS

Sample	Peak at low temperature	Peak at high temperature	Acidity (mmol/g)
1 wt% ZrO_2/MoO_3	220.4	636.1	0.043
10 wt% ZrO_2/MoO_3	–	533.0	0.080

FESEM studies: The morphological feature and particle size of prepared zirconia supported on molybdenum oxide catalysts calcined at 500 ºC can be obtained from field emission scanning electron microscope (FESEM) analysis. The results showed that the ZrO_2 loading over MoO_3 catalyst were agglomerated and aggregated each other on the surface which form rough surface morphology. FESM micrographs of 1ZM and 10ZM samples are shown in Fig. 6.

The 1ZM catalyst showed a rod shaped while 10ZM catalyst showed somewhat distorted shaped nature with agglomeration and both were in nanocrystalline nature. To investigate the presence of different element in prepared ZM catalysts, EDX analysis was carried out for all prepared catalysts and indicated the composition of the sample in Fig. 7.

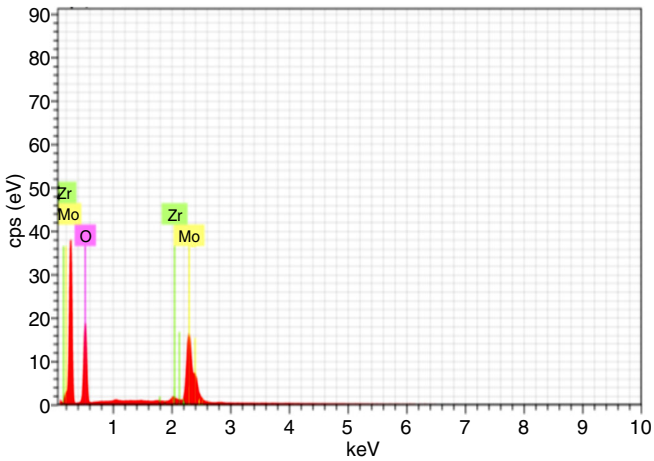

Fig. 7. EDX analysis of 1 ZM sample

TEM studies: The TEM images of ZrO_2 and ZrO_2/MoO_3 catalysts are shown in Fig. 8. The images confirmed the formation of spherical morphology with uniform size and shape. The average particle size obtained from TEM was found to be

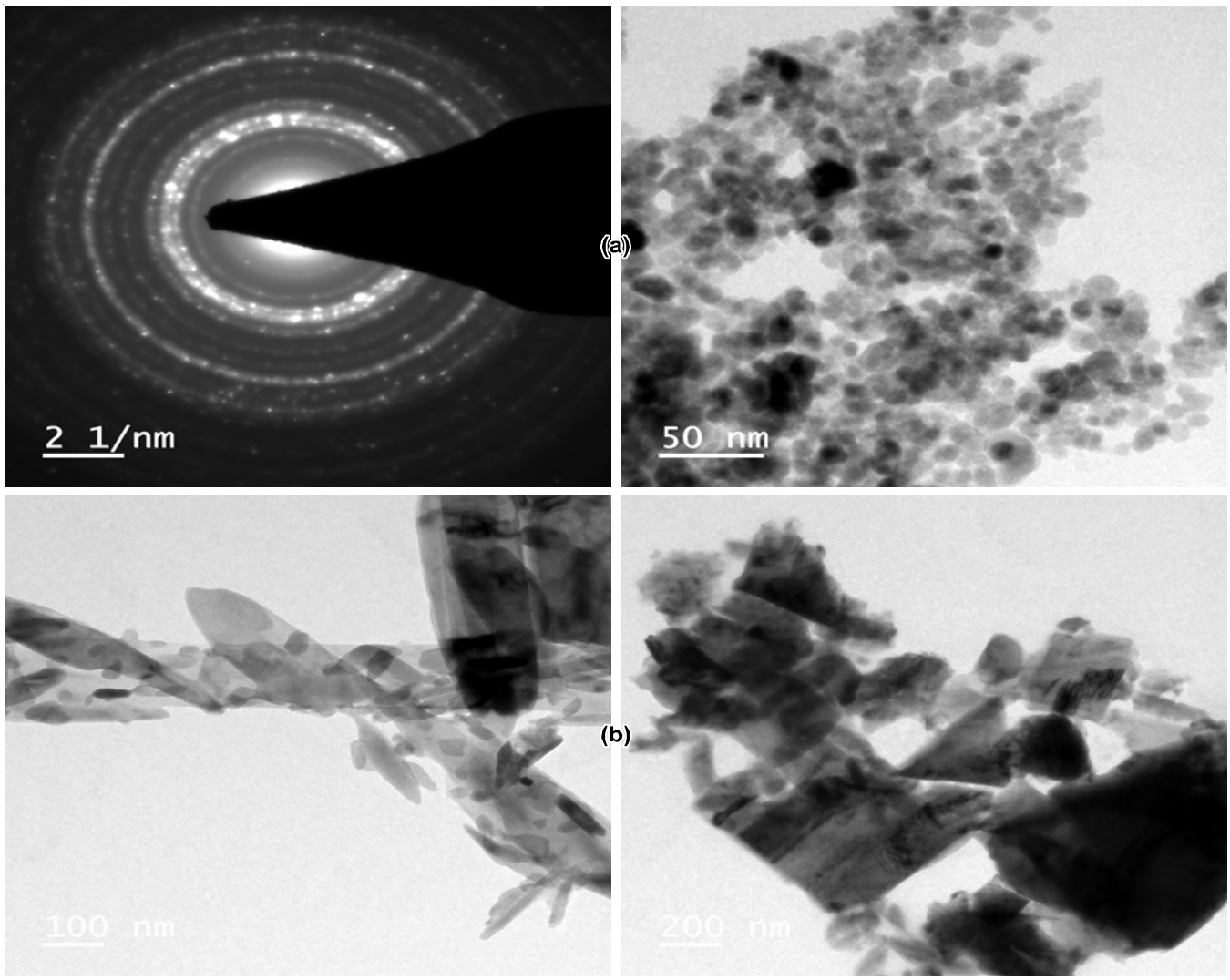

Fig. 8. TEM micrographs of (A) 1ZM and (B) 10ZM samples

in the range 6-20 nm, which is in good agreement with results obtained by XRD data. Pure ZrO_2 showed spherical and uniform sized particles but after the addition of MoO_3, the surface morphology of the sample changed to rod shaped particles with agglomeration. The results also point out that the synthesized samples were slightly agglomerated and the particles are somewhat uniform in size and shape.

XPS studies: The synthesized catalysts were investigated by XPS technique to study the oxidation state of the elements present in prepared samples. The photoelectron peaks of Zr 3*d*, Mo 3*d*, and O 1*s* are shown in Fig. 9, which clearly indicate that the XPS bands depend on zirconia coverage in MoO_3 oxide conveyor. The binding energies of the respective orbitals present in ZM catalysts are shown in Table-3.

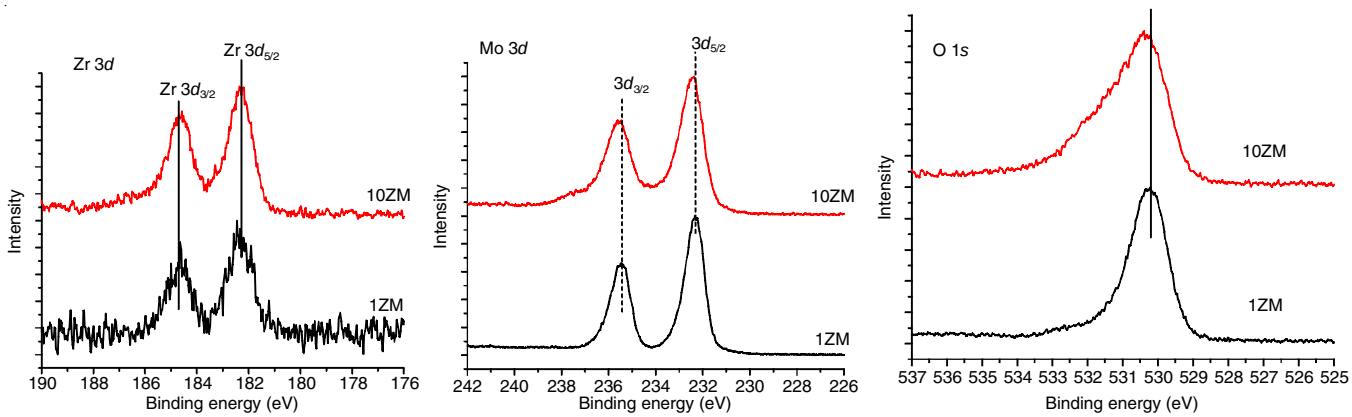

Fig. 9. Zr 3*d* (a); Mo 3*d* (b) and O 1*s* (c) XPS spectra of ZM catalysts

TABLE-3
BINDING ENERGIES (eV) OF THE PREPARED CATALYSTS

Sample	O 1s	Zr $3d_{3/2}$	Zr $3d_{5/2}$	Mo $3d_{3/2}$	Mo $3d_{5/2}$
1 wt% ZrO_2/MoO_3	530.4	182.35	184.65	232.36	235.5
10 wt% ZrO_2/MoO_3	530.69	182.36	184.66	232.52	235.6

Zr 3*d*: The core level spectra of Zr 3*d* in ZrO_2/MoO_3 samples are present in Fig. 9a. Two peaks were observed which can be concerned to the binding energy of Zr $3d_{3/2}$ and Zr $3d_{5/2}$ at 184.4 and 182eV respectively, these peaks are characteristic of Zr^{4+} species. The binding energies (BE) difference between the Zr $3d_{5/2}$ and Zr $3d_{3/2}$ photoemission feature is 2.4 eV, which was well matched with the literature [17]. The peaks become more sharp with increased in the zirconia loading.

Mo 3*d*: The energy line of Mo 3*d* core levels is shown in Fig. 9b. The ZM samples showed binding energy of Mo $3d_{3/2}$ and Mo $3d_{5/2}$ level at around 232.36 ± 0.1 and 235.5 ± 0.1 eV, respectively, correspond to the oxidation state of Mo(VI), which confirmed that Mo is in oxidic MoO_3 phase [18]. The results showed that the binding energy of Mo 3*d* slightly increased with increase in Zr loading. This increases in binding energy may be due to the increase inloading of zirconia on molybdenum and also may due to the formation of new phases.

O 1*s*: The energy line of the O 1*s* core levels is showed in Fig. 9c. The binding energy of O 1*s* in 1 wt% ZM catalyst is 530.4 eV, while in 10 wt. % ZM, increased in binding energy of O 1*s* to 530.69 eV were observed, which is attributed due to the overlapping contribution of oxygen from zirconia and molybdenum [19].

The XPS analysis was carried out to obtain data on the surface structure and the dispersion of the active phases present in the synthesized catalysts. The calculated surface atomic ratios for 1ZM and 10 ZM samples are summarized in Table-4.

TABLE-4
ELEMENTAL SURFACE CONTENT OF THE PREPARED CATALYSTS MEASURED BY XPS

Sample	Element content (at %)			
	O	Mo	C	Zr
1 wt% ZrO_2/MoO_3	43.2	22.71	33.5	0.491
10 wt% ZrO_2/MoO_3	46.63	18.25	31.14	3.955

Catalytic activity: The catalytic activities of synthesized ZrO_2/MoO_3 catalysts were determined by the condensation reaction of dibenzoyl methane and phenyl hydrazine at varied reaction parameters. The reaction was performed in two necked 50 mL round bottom flask kept in sonicator for 30 min under solvent free condition. In typical run, a mixture of dibenzoyl methane and phenyl hydrazine (1:1 molar ratio) with 0.25 g of ZM catalyst (activated at 200 ºC for 2 h) were carried out in ultrasonicator. The reaction was monitored by TLC, after completion of the reaction, the reaction mixture was filtered to recover the catalyst, the product was recrystallized from alcohol.

Defferent parameter were studied to optimize the reaction condition such as effect of temerature, various catalysts and solvents as follows:

Optimization of reaction conditions: The different conditions on the condensation rate of dibenzoyl methane and phenylhydrazine on synthesized catalysts is shown in Table-5. The best results were obtained, when a reaction was conducted without solvent in a sonicator with a yield of 97.7%. The suggestion that sonication uses sound waves to stir the particles in a reaction mixture and converts an electrical signal into a physical vibration to separate the substances. These interruptions can mix solutions, accelerate the dissolution of a solid into a liquid, such as sugar in water and eliminate the dissolved gas from the liquids. All the reactions gave 100% product selectivity. Therefore, the ultrasonic condition was optimized for the subsequent reaction.

TABLE-5
OPTIMIZATION OF CONDITION REACTION

Entries	Catalysts	Solvents	Conditions	Time (min)	Yield (%)
1	1ZM	Acetonitrile	Reflux	60	97.0
2	1ZM	Solvent-free	Granding	30	42.7
3	1ZM	Solvent-free	R.T	30	83.7
4	1ZM	Solvent-free	60 °C	30	82.5
5	1ZM	Solvent-free	Sonicator	30	97.7

Reaction condition: Dibenzoyl methane (1 mmol) , phenyl hydrazine (1 mmol), 0.25 g of catalyst.

To study the choice of catalyst, condensation of dibenzoyl methane and phenylhydrazine was carried out to form substituded pyrazole. Initially, the reaction was conducted in the absence of catalyst and observed that the condensation did not work satisfactorily. Thus, the above reaction was conducted separately in the presence of different catalysts such as ZrO_2, 1 wt.% ZrO_2/MoO_3 and 10 wt.% ZrO_2/MoO_3, the results are summarized in Table-6. The maximum yield (97.7%) was obtained when the reaction was carried out in the presence of a 1ZM catalyst, which could be the optimal acidity required for the condensation reaction in the presence of catalyst.

TABLE-6
REACTION USING VARIOUS CATALYSTS

Entry	Substrate	Catalyst	Yield (%)
1	Phenyl hydrazine	Without catalyst	No reaction
2		ZR	72.0
3		1ZM	97.7
4		10ZM	98.0
5	Hydrazine hydride	Without catalyst	No reaction
6		ZR	75.0
7		1ZM	70.0
8		10ZM	73.0

To investigate the choice of solvent, the reaction was carried out by using defferent solvents such as ethanol, acetonitrile, ethyl acetate, chloroform and water were used in the reaction at 60 ºC under optimized condition as shown in Table-7. From results, it was found that the reactions in acetonitrile and ethyl acetate showed good yeilds of pyrazole derivatives as compared to the other solvents.

To highlight the advantages of this proceses, the efficiency of synthesis of substituted pyrazoles was compared using present process with other methods reported in the literatures as shown in Table-8. Each of these method has their own advantages over others, but using of ZrO_2/MoO_3 catalyst in sonicator

TABLE-7
REACTION USING VARIOUS SOLVENTS

Entry	Solvents	Temp. (°C)	Time (min)	Yield (%)
1	Chloroform	60	120	76.50
2	Ethylacetate	60	120	93.18
3	Ethanol	60	60	–
4	Water	60	240	90.00
5	Acetonitrile	60	120	93.30

Reaction condetion: Dibenzoyl methane (1 mmol), hydrazine (1 mmol), 0.25 g of 1ZM catalyst

under solvent free condition as shown in this protocol could be a new substitutional in the green and economical synthesis of substituted pyrazoles.

Reusability studies: The reusability of zirconia supported catalyst was examined under optimized condition,the activity of zirconia catalysts was almost constant in recycle experiments and showed the suitability of catalyst for the condensation of dibenzoyl methane and hydrazine as shown in Fig. 10. The catalyst was easily separated from reaction mixture by filtration after completion of reaction, washed and heated at 500 ºC for 3 h and subjected to the next catalytic run with same reaction conditions.

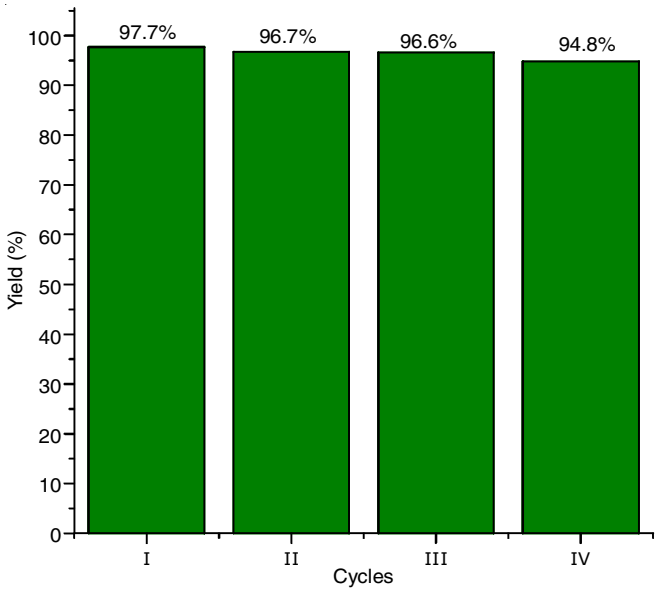

Fig. 10. Reusability efficiency data of 1ZM sample; Reaction condetion: Dibenzoyl methane (1 mmol), hydrazine (1 mmol), 0.25 g of 1ZM catalyst in sonicator for 30 min

After recycle and reuse of 1% ZrO_2/MoO_3 catalyst, the results showed that slight decrease in yield (from 97.7 to 96.7%) tooke place. From the data, it was clear that catalyst gave good stability and recycled three times without significant lose of its activity.

Spectral data: Substituted pyrazoles were identified by comparing FTIR, ^{1}H NMR and melting point data with the values reported in the literature [25,26].

1,3,5-Triphenyl-pyrazole: m.p.: 137-138 ºC; FT-IR (KBr, ν_{max}, cm^{-1}): 1595, 1494, 1455, 1362, 971, 920, 762, 666, 597. ^{1}H NMR (500 MHz, $CDCl_3$): 6.87 (s, 1H), 7.26 (m, 13H), 7.97 (d, 2H).

3,5-Diphenyl-1*H*-pyrazole: m.p.: 200-201 ºC; FT-IR (KBr, ν_{max}, cm^{-1}): 1660, 1572, 1405, 1271, 1179, 1673, 1025, 999, 974, 915, 750, 687. ^{1}H NMR (500 MHz, $CDCl_3$): 6.87 (s, 1H), 7.49-7.54 (m, 6H), 7.9 (d, 4H).

Conclusion

The ZrO_2/MoO_3 catalysts were synthesized using a sol-gel method and studied by a range of physico-chemical methods to reveal the impact of zirconia precursor, loading and thermal treatment temperature on the catalyst properties. The particle size of prepared samples were determined by XRD technique, which exhibited nanosized crystalline nature with average crystallite size in between 6.7-17 nm and concluded that synthesized ZrO_2 catalyst was mainly in tetragonal phase. After calcination at higher temperature, a mixture of tetragonal and monoclinic phases were observed and also the crystalline size increases with the increasing the calcination temperature. The structure of the synthesized catalysts was proved by the FT-IR data which showed the presence of metal-oxygen bonding. The Raman spectra of synthesized ZrO_2 catalyst showed the tetragonal phase of zirconia which well matched with XRD data, also Raman spectra of ZrO_2/MoO_3 catalyst showed presence of tetragonal phase of zirconia along with peaks corresponding to α-MoO_3. The acid strength and acid amount of synthesized catalysts were determined by TPD spectroscopy, in ZrO_2 sample, Strong desorption peak were observed at around 692 ºC which might be due to the surface Zr^{2+} species and OH^- species. The incorporation of zirconia into the molybdenum network has changed its surface acid properties due to the Zr^{2+} and Mo^{6+} ions, two different peaks was observed in ZM samples, the molybdenum showed only weak acid sites at low temperature region, therefor after addition of ZrO_2 on MoO_3, it showed the weak and strong acid sites. The FESEM analysis revealed the spherical shaped uniform particle size distribution and mesoporous structure. The EDX data confirmed the presence of elements in the synthesized catalysts. Therefore, the EDX confirmed the composition of ZrO_2 and ZrO_2/MoO_3 catalysts. The TEM images confirmed the formation of spherical morphology with uniform size and shape with slightly agglomeration. The XPS spectra determined the oxidation state of papered catalysts, the Zr 3*d* energy region of prepared catalysts showed two peaks which concerned to the binding energy of Zr $3d_{3/2}$ and Zr $3d_{5/2}$ at 184.4 and 182 eV, respectively, sharp

TABLE-8
COMPARISON OF OUR RESULTS WITH REPORTED RESULTS FOR SYNTHESIS OF 1,3,5-SUBSTITUTED PYRAZOLES

Entries	Catalysts	Solvents	Condition	Time (min)	Yield (%)	Ref.
1	Nano-TiO_2	Solvent free	R.T.	180	92	[20]
2	Nano-silica sulfuric acid	Solvent free	60 °C	30	95	[19]
3	[a-$Zr(CH_3PO_3)_{1.2}(O_3PC_6H_4SO_3H)$]	Solvent free	40 °C	120	95	[23]
4	1ZM	Solvent free	Sonicator	30	97.7	This work

peak were obtained with increasing in zirconia loading. The catalytic activity of the synthesized catalysts was tested over condensation reaction to synthesize substituted pyrazoles under mild conditions gave 97.7% yield of the products (1,3,5-triphenyl pyrazole/3,5-dephenyl-1*H*-pyrazole) condensation of dibenzoyl methane and phenylhydrazine. The advantages of the present study were short reaction times, simple operational procedure, good yield of all reactions and purification of products by recrystallization. Reuse of the catalyst for four times with almost same results indicate its reusability and stability.

CONFLICT OF INTEREST

The authors declare that there is no conflict of interests regarding the publication of this article.

REFERENCES

1. J.C. Védrine, *Catalysts*, **7**, 341 (2017); https://doi.org/10.3390/catal7110341
2. M.S. Khayoon and B.H. Hameed, *Appl. Catal. A: Gen.*, **466**, 272 (2013); https://doi.org/10.1016/j.apcata.2013.06.044
3. C. An, Y. Zhang, H. Guo and Y. Wang, *Nanoscale Adv.*, **1**, 4644 (2019); https://doi.org/10.1039/C9NA00543A
4. S. Fang, D. Bresser and S. Passerini, *Adv. Energy Mater.*, **10**, 1902485 (2020); https://doi.org/10.1002/aenm.201902485
5. Y. Zhu,, Q. Lin, Y. Zhong, H.A. Tahini,, Z. Shao and H. Wang, *Energy Environ. Sci.*, **13**, 3361 (2020); https://doi.org/10.1039/D0EE02485F
6. F. Haque, T. Daeneke, K. Kalantar-Zadeh and J.Z. Ou, *Nano-Micro Lett.*, **10**, 23 (2018); https://doi.org/10.1007/s40820-017-0176-y
7. C. Rodenbücher and K. Szot, *Crystals*, **11**, 256 (2021); https://doi.org/10.3390/cryst11030256
8. K. Yuan, X. Jin, Z. Yu, X. Gan, X. Wang, G. Zhang, L. Zhu and D. Xu, *Ceram. Int.*, **44**, 282 (2018); https://doi.org/10.1016/j.ceramint.2017.09.171
9. X. Dong, F. Li, N. Zhao, F. Xiao, J. Wang and Y. Tan, *Appl. Catal. B*, **191**, 8 (2016); https://doi.org/10.1016/j.apcatb.2016.03.014
10. Z. Liu, H. Su, J. Li and Y. Li, *Catal. Commun.*, **65**, 51 (2015); https://doi.org/10.1016/j.catcom.2015.02.028
11. Z. Li, C. Liu, X. Zhang, W. Wang, B. Wang and X. Ma, *Kinet. Catal.*, **59**, 481 (2018); https://doi.org/10.1134/S0023158418040055
12. S. Kemdeo, *Bull. Chem. React. Eng. Catal.*, **7**, 92 (2012); https://doi.org/10.9767/bcrec.7.2.3521.92-104
13. M. Benjaram Reddy, B. Chowdhury, E.P. Reddy and A. Fernández, *J. Mol. Catal.*, **162**, 431 (2000); https://doi.org/10.1016/S1381-1169(00)00336-8
14. M.R. Dumont, E.H.M. Nunes and W.L. Vasconcelos, *Ceram. Int.*, **42**, 9488 (2016); https://doi.org/10.1016/j.ceramint.2016.03.021
15. M.A. Shadiya, N. Nandakumar, R. Joseph and K.E. George, *Adv. Powder Technol.*, **28**, 3148 (2017); https://doi.org/10.1016/j.apt.2017.09.029
16. H.J. Lee, D.-C. Kang, S.H. Pyen, M. Shin, Y.-W. Suh, H. Han and C.-H. Shin, *Appl. Catal. A Gen.*, **531**, 13 (2017); https://doi.org/10.1016/j.apcata.2016.11.032
17. B.S. Rathod, M.K. Lande, B.R. Arbad, A.B. Gambhire, *Arab. J. Chem.*, **7**, 253 (2014); https://doi.org/10.1016/j.arabjc.2010.10.027
18. C. Liu, W. Wang, Y. Xu, Z. Li, B. Wang and X. Ma, *Appl. Surf. Sci.*, **441**, 482 (2018); https://doi.org/10.1016/j.apsusc.2018.02.019
19. A. Calafat, L. Avilán and J. Aldana, *Appl. Catal. A Gen.*, **201**, 215 (2000); https://doi.org/10.1016/S0926-860X(00)00441-5
20. W. Shi, H. Liu, D. Ren, Z. Ma and W. Sun, *Chem. Res. Chin. Univ.*, **22**, 364 (2006); https://doi.org/10.1016/S1005-9040(06)60117-7
21. F.N. Seyed, H. Nikkhah and A. Elhampour, *Chinese Chem. Lett.*, **26**, 1397 (2015); https://doi.org/10.1016/j.cclet.2015.07.009
22. X. Chen, C. Huang, Y. Shi, B. Yuan, Y. Sun and Z. Bai, *Powder Technol.*, **344**, 581 (2019); https://doi.org/10.1016/j.powtec.2018.12.056
23. C. Ranga, R. Lødeng, V.I. Alexiadis, T. Rajkhowa, H. Bjørkan, S. Chytil, I.H. Svenum, J. Walmsley, C. Detavernier, H. Poelman, P. Van Der Voort and J.W. Thybaut, *Chem. Eng. J.*, **335**, 120 (2018); https://doi.org/10.1016/j.cej.2017.10.090
24. P. Bhaumik, T. Kane and P.L Dhepe, *Catal. Sci. Technol.*, **4**, 2904 (2014); https://doi.org/10.1039/C4CY00530A
25. S. Samantaray, G. Hota and B.G. Mishra, *Catal. Commun.*, **12**, 1255 (2011); https://doi.org/10.1016/j.catcom.2011.04.014
26. K. Aghapoor, L. Ebadi-Nia, F. Mohsenzadeh, M.M. Morad, Y. Balavar and H.R. Darabi, *J. Organomet. Chem.*, **708-709**, 25 (2012); https://doi.org/10.1016/j.jorganchem.2012.02.008